Materials Science and Engineering C 29 (2009) 819–822

Contents lists available at ScienceDirect

Materials Science and Engineering C

journal homepage: www.elsevier.com/locate/msec

Polymer-assisted synthesis of hydroxyapatite nanoparticle

Yao-Hsuan Tseng [a,*], Chien-Sheng Kuo [b], Yuan-Yao Li [b], Chin-Pao Huang [c]

[a] Department of Chemical Engineering, National Taiwan University of Science and Technology, Taipei, 106, Taiwan, ROC
[b] Department of Chemical Engineering, National Chung Cheng University, Chia-Yi, 621, Taiwan, ROC
[c] Department of Civil and Environmental Engineering, University of Delaware, Newark, Delaware, 19716, USA

ARTICLE INFO

Article history:
Received 26 November 2007
Received in revised form 3 July 2008
Accepted 24 July 2008
Available online 30 July 2008

Keywords:
Nano-hydroxylapatite
One-step process
Polyethylene glycol

ABSTRACT

Hydroxyapatite (HA, $Ca_{10}(PO_4)_6(OH)_2$) nanoparticles were synthesized using calcining calcium dihydrogenphosphate ($Ca(H_2PO_4)_2 \cdot H_2O$), calcium hydroxide ($Ca(OH)_2$), and polyethylene glycol (PEG) at 900 °C in an oxygen atmosphere. This one-step process yields HA nanoparticles with similar particle sizes (e.g., 50–80 nm) that are well-crystallized and non-aggregated. PEG is an important factor in controlling the particle size, crystal phase, and degree of aggregation in these HA particles. This conclusion is supported by results from a field-emission scanning electron microscope (FE-SEM), X-ray diffractometry (XRD), energy dispersive X-ray analysis (EDS), a high-resolution transmission electron microscope (HR-TEM), and dynamic light scattering (DLS).

1. Introduction

Synthetic hydroxyapatite, $Ca_{10}(PO_4)_6(OH)_2$, is a bioactive material that is chemically compatible with biological apatite, the mineral constituent of hard human tissues such as bones and teeth [1–3]. With excellent biocompatibility and bioactivity, hydroxyapatite has been widely used in medical, dental, and other health-related fields as material for damaged bones or teeth, important implant and scaffold materials, and drug delivery agents [4–5]. With their high area to volume ratio, nano-sized HA particles are expected to be excellent materials for these applications. For this reason, researchers have developed many HA synthesis techniques, including sol-gel methods [6], co-precipitation [7], emulsion techniques [8–9], mechanochemical methods [10], electrochemical deposition [11], and hydrothermal processes [12]. However, none of these methods are feasible for large-scale industrial production processes because they involve expensive materials, complicated processes, serious aggregation (i.e., large particle size), wide-ranging particle size, and numerous impurities (e.g., undesired crystal phase, β-tri-calcium phosphate, TCP). In wet chemical synthesis (e.g. sol-gel), synthesis steps include gelation, aging, drying, and sintering. The aging and drying times are long, and require precisely controlled reaction conditions. Particles prepared by the sol-gel process usually aggregate seriously during sintering. The objective of this study is to develop an easy, inexpensive, and fast method of producing nano-sized HA particles with consistently high quality.

A previous study shows that polymers such as PEG (poly(ethylene glycol)) and PVP (polyvinyl pyrrolidone) are useful components in the formation of one- and zero-dimension nano-sized materials. Li and coworkers successfully prepared ZnO nanowires and nanorods using a short-chain PEG-assisted pathway [13]. Chirakkal et al. presented the polymer-assisted growth of molybdenum oxide whiskers [14]. Xiong et al. prepared Al_2O_3–TiO_2 composite nanoparticles using a sol-gel method with PEG as a gelling agent [15]. Polymeric materials often serve as stabilizers for metal colloids, preventing their agglomeration and precipitation [16], i.e. steric stabilization. Due to the ether oxygen groups with rich electrons in its chain, PEG is able to form complexes with metal cations and enhance the homogeneous mixing of metal cations [17]. Metal cations can easily disperse in a solution at the

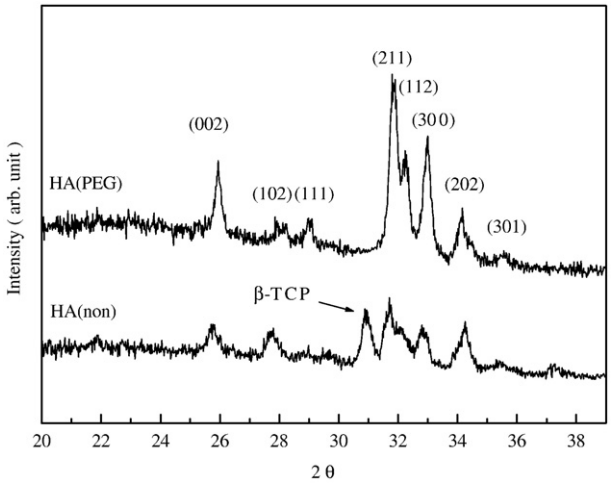

Fig. 1. X-ray powder diffraction patterns of the synthesized HA nano-particles.

* Corresponding author. Tel.: +886 2 27376765; fax: +886 2 27376644.
E-mail address: tyh@email.ntust.edu.tw (Y.-H. Tseng).

0928-4931/$ – see front matter © 2008 Elsevier B.V. All rights reserved.
doi:10.1016/j.msec.2008.07.028

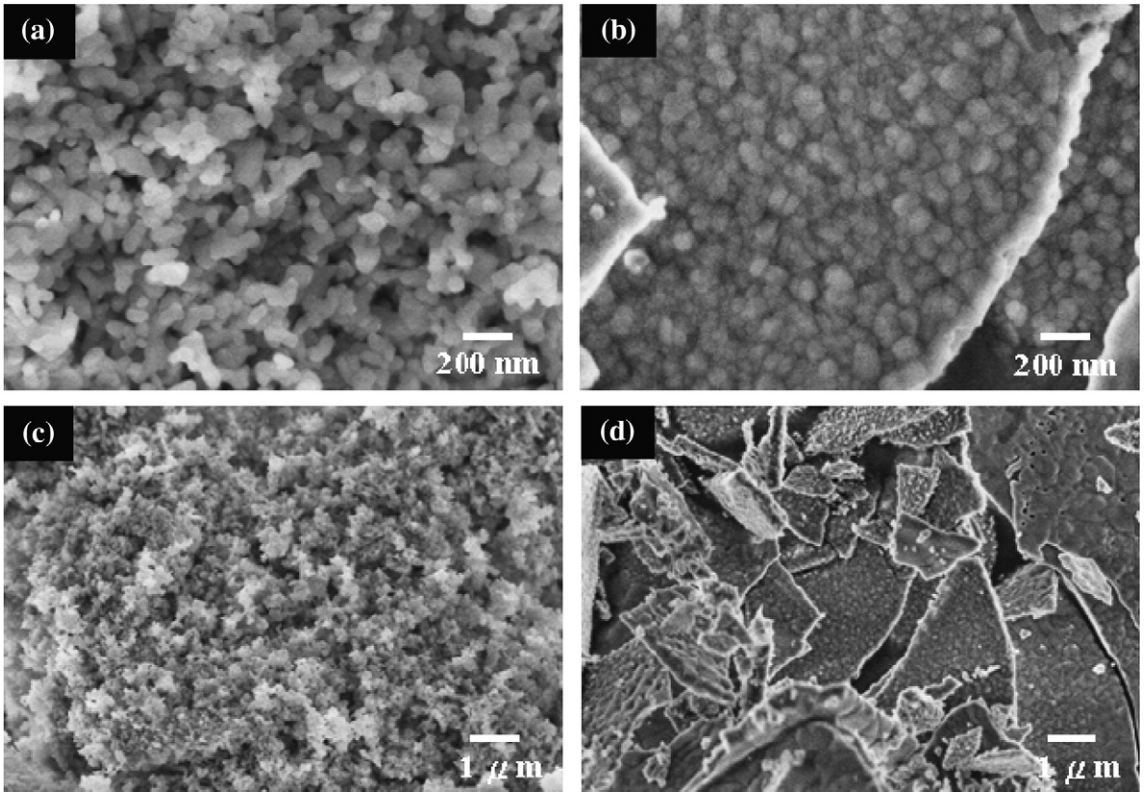

Fig. 2. FE-SEM morphology of synthesized nano-particles. (a) HA(PEG), (b) HA(non).

molecular level because of the interaction within, and random arrangement of, the polymer chain. Furthermore, interactions between PEG and metal cations change metal compound physical properties such as thermal stability and aggregation size.

This study reports a fast and inexpensive method of synthesizing HA nanoparticles using PEG. This one-step approach yields HA nanoparticles that are well-crystallized, highly dispersed, and have similar particle sizes. The properties of HA materials, such as their chemical composition, crystal phase, purity, and particle size, were determined by FE-SEM, XRD, EDS, HR-TEM, and DLS techniques.

2. Experimental

Dihydrogenphosphate and calcium hydroxide served as the sources of calcium and phosphorous for HA in this study. The Ca/P molar ratio was maintained at 1.67, the stoichiometric amount of HA ($Ca_{10}(PO_4)_6(OH)_2$). Exact amounts of dihydrogenphosphate (1.25 g), calcium hydroxide (0.85 g), and PEG (4 g, MW:20000) were measured and dissolved in 30-mL of de-ionized water and heated to 65 °C to facilitate PEG dissolution. The mixture was stirred for 30 min at 300 rpm, producing a milky gel suspension. This gel was then placed in a furnace and heated at 900 °C for 30 min under normal atmospheric conditions. This process produced a white hydroxypatite powder. The entire synthesis experiment was then repeated under the same conditions while excluding PEG. Sample labels were defined as HA(PEG) and HA (non) for HA particles prepared with and without PEG, respectively. The crystal structures were analyzed by X-ray diffraction (Shimadzu, XRD6000), and the 2θ-scan was recorded using Cu Kα radiation. Surface morphology was observed with a field-emission microscopy electron microscope (Hitachi, S4800), with energy dispersion spectroscopy (Horiba, EX-210) and high-resolution transmission electron microscopy (Philips, Tecnai F20). The aggregated particle size was determined by the DLS technique (Malvern, 3000HS) in an ethanol suspension (0.1 g of sample/100 mL of ethanol).

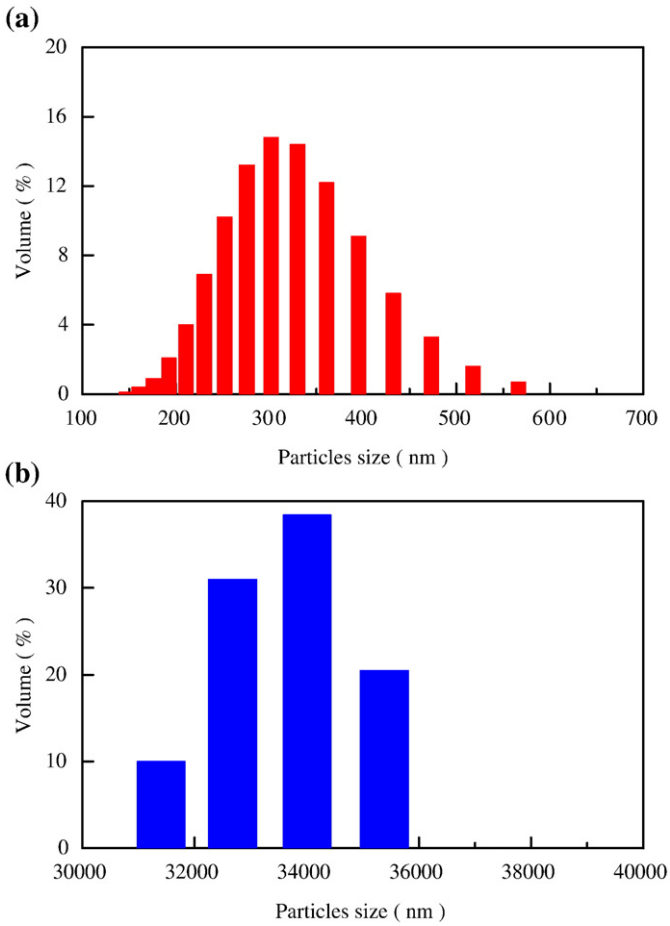

Fig. 3. Particle size analysis of synthesized HA nanoparticles using DLS. (a) HA(PEG), (b) HA (non).

3. Results and discussion

Fig. 1 shows the X-ray diffraction patterns of HA(PEG) and HA (non). The characteristic peaks at 2θ were 25.9° (002), 30.0° (102), 28.9° (111), 31.9° (211), 32.3° (112), 32.9° (300), 34.2° (202), and 35.4° (301) for HA(PEG) particles. According to the Joint Committee on Powder Diffraction Standards (JCPDS) database, these values indicate the presence of a pure hydroxyapatite structure. The HA(non) samples exhibited a somewhat different crystal phase than the pure hydroxyapatite. The variant peak at $2\theta = 30.9°$ of the HA(non) sample was referred to the β-TCP phase [18]. Wang et al. reported that the hydroxyapatite structure can be transformed into a β-TCP phase at a sintering temperature of 900 °C [18]. The β-TCP phase is a common impurity in HA material, and its presence can decrease the bioproperties of HA. However, using PEG effectively inhibits the production of β-TCP phase during HA preparation. This can be attributed in part to the heat energy consumed during the thermal decomposition of PEG. It is speculated that PEG effectively suppresses β-TCP phase formation during HA preparation because the decomposition of PEG and the crystallization of HA occur simultaneously during the calcination process at 900 °C. The energy for formation of HA structure in the HA(PEG) system is more than HA(non) because crystallization of HA will proceed after decomposition of PEG-Ca-P complex in former system. This effectively delays the phase transition from pure HA to the β-TCP phase. Therefore the undesired β-TCP phase does not form in polymer-assisted reactions at 900 °C in 30 min.

Fig. 2 (a) and (b) show the morphology of HA(PEG) and HA(non) particles, respectively. Fig. 2(a) shows that HA(PEG) exhibits a narrow size distribution, with an average particle size of 50–80 nm. Fig. 2(b) shows that the HA(non) particles had serious aggregation, larger particle sizes, and wider size distribution (80–150 nm) than HA(PEG). Low magnification SEM images clearly show the degree of aggregation. The HA(PEG) was well-dispersed, while the HA(non) was seriously aggregated into a single flat piece. Furthermore, the hydroxyapatite particle is usually dispersed in water and ethanol solution for coating application and mix with other biomaterials, so the good hydroxyapatite suspension should be slightly aggregated for convenient use. Hence, the hydroxyapatite ethanol suspensions were prepared for determination of their secondary particle sizes. The analysis of the ethanol solution using the DLS technique indicates that the diameter of HA(PEG) secondary particle sizes ranges from 150 to 600 nm) and that of HA(non) ranges from 35 to 36 μm), as Fig. 3 shows. Obviously, HA(PEG) was much less aggregated than HA(non). The particle with smaller primary particle size gives the smaller secondary particle size as shown in our present and previous works [19–21]. The secondary particle plays an important role in the physical–chemical properties of nano-particle, such as adhesion and catalytic activity. Tao et al. reported that the PEG polymer can inhibit

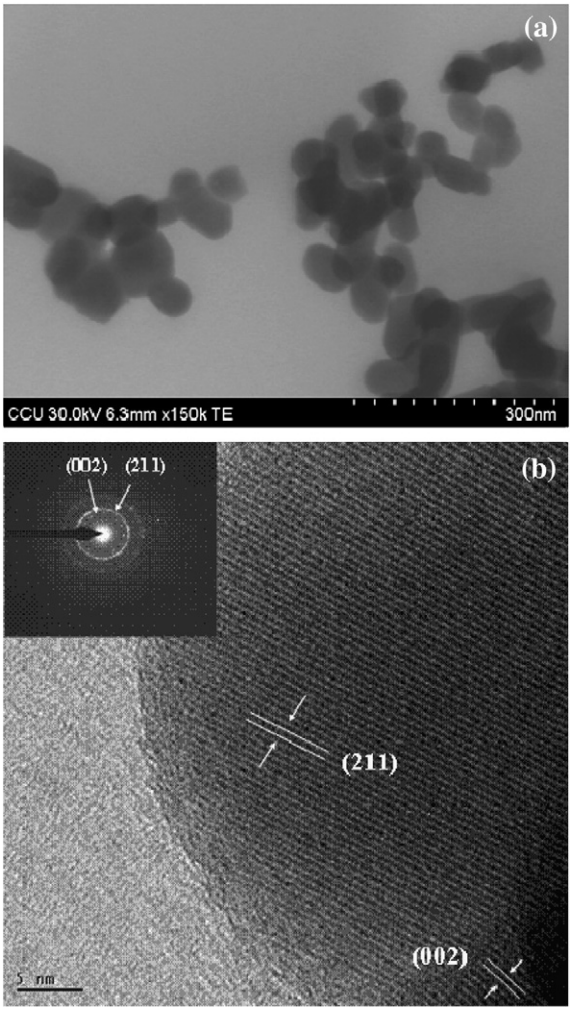

Fig. 5. TEM image of the HA(PEG) powder. (a) TEM, (b) HR-TEM with the selected area diffraction pattern (insert).

the assembly of nanoparticles [22]. Ether oxygen groups in the PEG were responsible for the lower aggregation level in HA(PEG). PEG molecules surround metal ions, Ca^{2+} in this case, to form small and well-dispersed nanoparticles.

Energy dispersive spectroscopy (EDS) was employed to investigate the elemental composition of HA. The results in Fig. 4 demonstrate that only Ca, P, and O appear in HA(PEG) samples. Also note that no other impurity, including carbonaceous species, was present in the HA nanoparticles. It depict the PEG compound is completely decomposed

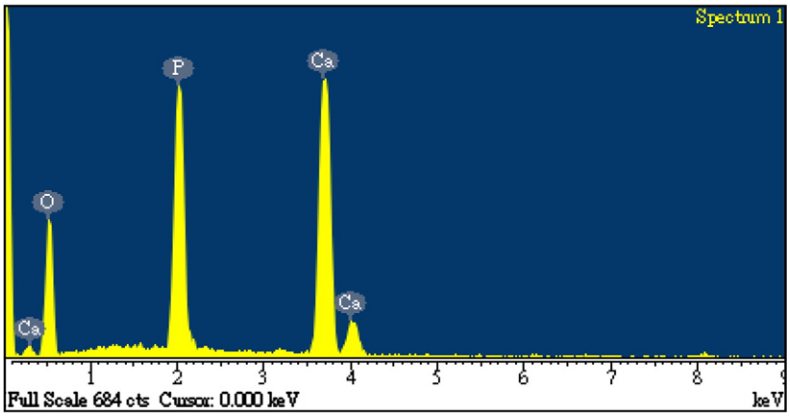

Fig. 4. EDS spectra of HA(PEG) nanoparticles.

to volatile compounds after calcination step as found in TG-MS analysis results (not shown). TG-MS results of HA(PEG) samples indicate that water (m(mass)/z(charge) = 18) was released continuously as the temperature increased. Other gas products such as hydrogen (m/z = 2), methane (m/z = 16), carbon monoxide (m/z = 28), and carbon dioxide (m/z = 44) started to appear as the temperature increased to about 400 °C, which reveals the PEG pyrolysis begins near 400 °C. These results agree well with those reported by Madorsky's and our previous works [23,24]. There are no carbonaceous gaseous products decomposed from the reactants of the HA(non) synthesis process.

Fig. 5(a) and (b) show the TEM and HR-TEM images of HA(PEG). HA nanoparticles exhibited a uniform particle size, which is consistent with the SEM images. Fig. 5(b) shows the HR-TEM image, and the insert is the selected area electron diffraction (SAED) pattern. The HA (PEG) particles were well-ordered structure with d-spacing of 0.2886 nm and 0.3502 nm in the crystalline phase, corresponding to the (211) and (002) planes of the HA structure. The result is consistent with the XRD patterns.

4. Conclusions

A simple PEG-assisted reaction was successfully developed for the preparation of HA nanoparticles. Well-ordered and uniform (50–80 nm) crystals composed of pure hydroxyapatite nanoparticles were obtained via one-step calcination of three cheap reactants, calcium dihydrogenphosphate, calcium hydroxide, and PEG. PEG played an important role in inhibiting particle aggregation and β-TCP phase generation during the polymer-assisted reactions. The barrier caused by PEG-Ca-P complex and decomposition of PEG provides calcium dihydrogenphosphate and calcium hydroxide a proper reaction condition for synthesis of small HA particles. The as-prepared HA nano-particle can be well-dispersed in solutions with small secondary particle size for convenient use and good bioactivity without impurity, β-TCP phase. In summary, this process offers a simple, economical, and potentially safe method for preparing HA nanoparticles.

References

[1] K.D. Groot, Biomaterials 1 (1980) 47.
[2] J.D. Currey, The Mechanical Adaptations of Bones, Princeton University Press, 1984.
[3] L.L. Hench, J. Am. Ceram. Soc. 74 (1991) 1487.
[4] R.Z. LeGeros, J. Oral Implantol. 28 (2002) 290.
[5] T.M. Chu, S.J. Hollister, J.W. Halloran, S.E. Feinberg, D.G. Orton, Ann. N. Y. Acad. Sci. 961 (2002) 114.
[6] A. Bigi, E. Boanini, K. Rubini, J. Solid State Chem. 177 (2004) 3092.
[7] Y.X. Pang, X. Bao, J. Eur. Ceram. Soc. 23 (2003) 1697.
[8] M.J. Phillips, J.A. Darr, Z.B. Luklinska, I. Rehman, J. Mater. Sci. Mater. Med. 14 (2003) 875.
[9] G.K. Lim, J. Wang, S.C. Ng, C.H. Chew, L.M. Gan, Biomaterials 18 (1997) 1433.
[10] W. Kim, Q.W. Zhang, F. Saito, J. Mater. Sci. 35 (2000) 5401.
[11] L.Y. Huang, K.W. Xu, J. Lu, J. Mater. Sci. Mater. Med. 11 (2000) 667.
[12] M. Yoshmura, H. Suda, K. Okmoto, K. Loku, J. Mater. Sci. 29 (1994) 3399.
[13] Z. Li, Y. Xie, Y. Xie, Inorg. chem. 42 (2003) 8105.
[14] C.V. Krishnan, J.G. Chen, C. Burger, B. Chu, J. Phys. Chem. B 110 (2006) 20182.
[15] G. Xiong, X. Wang, L. Lu, X. Yang, Y.F. Xu, J. Solid State Chem. 141 (1998) 70.
[16] D.H. Chen, Y.W. Huang, J. Colloid Interface Sci. 255 (2002) 299.
[17] T. Okada, Analyst 118 (1993) 959.
[18] F. Wang, M.S. Li, Y.P. Lu, Y.X. Qi, Mater. Lett. 59 (2005) 916.
[19] Y.H. Tseng, H.Y. Lin, C.S. Kuo, Y.Y. Li, C.P. Huang, Reac. Kinet.Catal. Lett. 89 (2006) 63.
[20] H. Lin, C.P. Huang, W. Li, C. Ni, S. Ismat Shah, Y.H. Tseng, Appl. Catal. B 68 (2006) 1.
[21] A.J. Maira, K.L. Yeung, C.Y. Lee, P.L. Yue, C.K. Chan, J. Catal. 192 (2000) 185.
[22] D.L. Tao, W.Z. Qian, Y. Huang, F. Wei, J. Crystal. Growth. 271 (2004) 353.
[23] S.L. Madorsky, S.J. Straus, J. Polym. Sci. 36 (1959) 183.
[24] C.W. Huang, Y.Y. Li, J. Phys. Chem. B 110 (2006) 23242.